Food & Function

ROYAL SOCIETY OF CHEMISTRY

PAPER

View Article Online
View Journal | View Issue

Cite this: *Food Funct.*, 2025, **16**, 7931

Pacific oyster (*Crassostrea gigas*) soft tissue extract attenuates TNF-α induced inflammation in a Caco-2 cell line

Mascia Benedusi,†[a] Martina Guerra,†[b] Giulia Trinchera,[b] Daniela Summa,[b] Francesco Chiefa,[c] Franco Cervellati,[a] Elena Tamburini,*[b] Luisa Pasti,[c] Giuseppe Castaldelli[b] and Giuseppe Valacchi*[b,d,e]

Marine food is well known to be rich in bioactive molecules that can aid in the prevention and treatment of chronic inflammatory diseases. Among them, bivalve mollusks such as the Pacific oyster (*Crassostrea gigas*) have been receiving growing interest due to their high nutritional and medicinal value. This study evaluated the chemical composition of Pacific oyster soft tissue extract (OE) and investigated its potential anti-inflammatory effects on human intestinal epithelial cells. The nutritional value including moisture, total protein, ash, total lipids, fatty acids (FAs), amino acids and minerals was analyzed, as well as polyphenol and carotenoid contents. The potential anti-inflammatory activity was tested at 5, 50, and 500 μg mL^{-1} concentrations of OE against TNF-α induced inflammation in the intestinal human epithelial cell line Caco-2. OE was shown to reduce both the TNF-α induced activation of the NF-κB pathway and the alteration of the epithelial barrier integrity. The present findings might provide evidence for further understanding how whole dried oyster meat can be developed as a low-cost nutraceutical dietary supplement and thus can offer a natural alternative to alleviate intestinal inflammation associated with different chronic diseases.

Received 2nd July 2025,
Accepted 30th August 2025

DOI: 10.1039/d5fo02637g

rsc.li/food-function

Introduction

Inflammation is the body's immune response against a variety of harmful agents, including pathogens, damaged cells, and toxins, which potentially can cause tissue injury or disease.[1] Inflammatory reactions are, therefore, a defence mechanism that acts by removing the damaging stimulus and inducing repair and recovery processes in injured tissues, through the activation of a biochemical signalling cascade. These signals activate leukocytes that produce transcription factors and pro-inflammatory cytokines leading to an inflammatory state.[2] Whereas a normal inflammatory response is characterized by the temporally restricted regulation of an inflammatory activity that occurs only in the presence of a threat and resolves once the threat has been eliminated, uncontrolled and prolonged inflammation can contribute to a variety of chronic diseases, such as cancer, diabetes, and cardiovascular diseases.[3]

An unhealthy diet is one of the primary causes of increased risks of developing chronic inflammatory diseases.[4] Components of certain foods and beverages, such as fats and alcohol, once ingested are known to trigger innate immune responses with serious implications such as chronic inflammation and permanent gut mucosal alterations.[5] Changes in the microbiota and intestinal permeability allow gut-derived toxins to cross the intestinal barrier, resulting in the overproduction of inflammatory cytokines.[6] These cytokines ultimately cause inflammation-related injury and eventually a systemic inflammatory condition.[7] In contrast, several epidemiological studies have demonstrated that inflammation may be prevented through the adoption of dietary patterns, foods, and bioactive compounds with protective anti-inflammatory properties. For this reason, an appropriate diet could represent a crucial exogenous aid for the prevention and treatment of chronic inflammatory diseases.[8]

It is widely acknowledged that phytochemicals from fruits, vegetables, and food legumes exhibit substantial anti-inflam-

[a]*Department of Neurosciences and Rehabilitation, University of Ferrara, Ferrara, Italy. E-mail: mascia.benedusi@unife.it, martina.guerra@unife.it, franco.cervellati@unife.it*
[b]*Department of Environmental and Prevention Sciences, University of Ferrara, Ferrara, Italy. E-mail: guerramartina0898@gmail.com, tme@unife.it, ctg@unife.it, vlcgpp@unife.it, daniela.summa@unife.it; Tel: +39 0532 455172, +39 0532 455482*
[c]*Department of Chemical, Pharmaceutical and Agrarian Sciences, University of Ferrara, Ferrara, Italy. E-mail: francesco.chiefa@unife.it, psu@unife.it*
[d]*Department of Animal Science, Plants for Human Health Institute, North Carolina State University, Kannapolis, NC, USA*
[e]*Department of Food and Nutrition, Kyung Hee University, Seoul, South Korea. E-mail: giuseppe.valacchi@unife.it*
†These authors contributed equally.

matory activities, such as polyphenols, polysaccharides, triterpenoids, and galactolipids.[9] On the other hand, in recent years, there has been a remarkable increase in pharmacological research on anti-inflammatory marine biomolecules as potential candidates for new drug discovery, and in general for the field of marine biotechnology. Marine fish, such as salmon, trout, tuna, and sardines, are well known to be rich in polyunsaturated fatty acids, molecules that are able to modulate the inflammatory process through the production of eicosanoids.[10]

In recent times, there has been growing interest in organisms belonging to the class Bivalvia, due to a range of different bioactive secondary metabolites that, under the pressure of natural selection, may have evolved.

The Pacific oyster (*Crassostrea gigas*) is the most widely farmed and consumed saltwater bivalve mollusc worldwide.[11] Marketed as live, frozen, or processed seafood, this species originates from Japan, and has now spread to both the northern and southern hemispheres.[12] In addition to being highly nutritious, oysters are a low-calorie, low-cholesterol source of protein and an exceptional source of zinc, which strengthens the immune system. Moreover, they are a rich source of bioactive compounds, with a wide range of biological activities that exert beneficial effects on human health.[13] A large body of literature reported the high nutritional value and bioactive compounds of *C. gigas*, such as peptides, polysaccharides, polyphenols and lipids, along with its bioactivity, including antimicrobial, antioxidant, antihypertensive, anticoagulant, anticancer, immunostimulating, antiwrinkle, antithrombotic and osteogenic effects.[14]

Recent studies have shown that purified oyster peptides and protein hydrolysates exert robust anti-inflammatory effects by suppressing pro-inflammatory cytokines.[15] For example, the tyrosine–alanine (Tyr–Ala) dipeptide, a multifunctional oyster-derived peptide, has demonstrated anti-inflammatory effects in an acute liver failure mouse model by reducing the activity of the nuclear factor kappa-light-chain-enhancer of activated B cells (NF-κB) and the mitogen-activated protein kinase (MAPK) pathways. The low-molecular-weight polypeptide β-thymosin derived from the mantle of *C. gigas* has proven *in vitro* anti-inflammatory activity in lipopolysaccharide (LPS)-induced RAW264.7 macrophage cells, inhibiting the nuclear translocation of NF-κB and its associated signalling pathway.[16,17] Moreover, Qian *et al.*[18] demonstrated the anti-inflammatory effects of four peptides (PEP-1, PEP-2, TRYP-2, and MIX-2) isolated from oyster soft tissue, by downregulating the tumor necrosis factor (TNF-α) and the mRNA expression of pro-inflammatory mediators (IL-1β, IL-6, and iNOS) in LPS-stimulated RAW264.7 cells. So far, no studies have evaluated the anti-inflammatory activities of *C. gigas in vivo.*

This study aimed to evaluate the chemical composition and nutritional value of Pacific oysters farmed in north-eastern Italy. Then, the potential protective effects of oyster soft tissue extract on human intestinal mucosa were explored by establishing the anti-inflammatory activities against TNF-α-induced inflammation in the Caco-2 cell line. The characterization of the specific bioactive compound potentially responsible for the bioactivity was performed based on the chemical composition and literature data. As an innovative contribution, this study analysed the potential anti-inflammatory activity of the extract of whole dried oyster soft tissue using a pro-inflammatory *in vitro* model. The present findings might provide evidence for further understanding of how whole dried oyster meat can be developed as a low-cost nutraceutical dietary supplement and thus provide a natural alternative for both the prevention and treatment of inflammatory injury.

Experimental

Pacific oysters used in this study were sampled in Goro, in the Po River delta on the north-eastern coast of Italy. 40 commercial-sized oysters (with an average weight of about 80 g) were collected. Immediately after harvesting, soft tissue was carefully separated from the shell, weighed, and stored by freezing at −80 °C until use. Approximately 10 commercial-sized individuals were freeze-dried (M. CHRIST, Alpha 1–2 LDplus, Osterode am Harz, Germany) and used for the analysis of chemical and nutritional composition, as well as for the determination of fatty acids, minerals and amino acid profiles. At the time of the assay, the samples were freeze-dried (Lyovapor L-200™, Buchi, Switzerland) and resuspended in absolute ethanol at a concentration of 100 mg mL^{-1}. The ethanolic extract was prepared as follows. An aliquot of 100 mg of freeze-dried oyster was transferred into a 2 mL Eppendorf tube, and 1 mL of absolute ethanol was added. The material was homogenized by maceration with a sterile pestle and intermittently vortexed for approximately 30 minutes to enhance extraction efficiency. The tube was then subjected to ultrasonic treatment in a water bath (Elma Transonic T 310; F. Franceschi Srl, Pisa, Italy) at room temperature for 30 minutes. This extraction cycle was repeated twice. Subsequently, the suspension was centrifuged at 3500 rpm for 15 minutes, and the supernatant was carefully separated from the insoluble residue. The resulting ethanolic extract was then used for Caco-2 cell treatments at different concentrations.

Chemical composition and nutritional value

The moisture content was determined by blending and freeze-drying the samples at −60 °C and 0.090 mbar. The results were expressed as a percentage. The protein content was determined on 0.6 g of freeze-dried sample, according to the Kjeldahl method.[19] The protein content was determined by means of a conversion factor equal to 6.25 and expressed as a percentage of wet mass (WM). The ash content was determined in 1 g of freeze-dried sample, in a muffle furnace at 570 °C (Z1200, Zetalab, Padova, Italy) overnight.[20] The total ash content was expressed as a percentage of WM. For lipid extraction, 1.5 g of freeze-dried product was placed in a thimble connected to a Soxhlet extraction unit (Velp Scientifica, Usmate, Milan, Italy). 50 mL of diethyl ether (Carlo Erba Reagents S.r.l, Milan, Italy) was used as the extraction

solvent. The extraction steps consisted of 30 min with a thimble immersed in boiling solvent, 30 min of reflux washing, and 10 min of solvent recovery.[21] Total lipids were expressed as a percentage of WM.

Fatty acid profile. After extraction by the Soxhlet method, fats were dissolved in 3 mL of hexane (Carlo Erba Reagents S.r.l), and transesterified with 1.5 mL of 5% sodium hydroxide in methanol (Carlo Erba Reagents S.r.l) to obtain free fatty acid methyl esters. 1 μL of sample was injected into a gas chromatography-mass spectrometry system (Varian Saturn 2100 MS/MS ion trap mass spectrometer coupled to a Varian 3900 gas-chromatograph, Varian, Palo Alto, CA, USA). The separation was achieved with a capillary column Zebron ZB-WAX (Phenomenex (60 m, 0.25 mm i.d., 25 μm film thickness, Milan, Italy)) supplied with a helium carrier gas at a constant flow of 1 mL min^{-1}. The injector temperature was set to 260 °C and the oven temperature program is as follows: start 100 °C for 2 min, rise to 200 °C at 10 °C min^{-1} and hold for 58 min. MS acquisitions were performed by electron ionization (EI), full scan mode, mass range, *m*/*z* 40–650 and the collected data were evaluated using the NIST MS library.[21]

Analysis of minerals. Sample mineralization had occurred in an Ethos Easy Advanced Microwave Digestion System equipped with an SK15 rotor (Milestone S.r.l., Sorisole, Italy). About 0.4 g of each oyster sample was weighed in a tetrafluoro-methoxyl vessel and was added with 9 mL of HNO_3 (69%, Suprapur®, Merck, Darmstadt, Germany) and 1 mL of H_2O_2 (30%, Carlo Erba Reagents). The microwave program consisted of heating for 15 minutes to 200 °C, followed by a holding time of 15 minutes at a maximum power of 1800 W. Mineralized samples were then filtered (ashless filters, Whatman 589/2) into a volumetric flask and filled until 50 mL with ultrapure water (MilliQ®, Merck KGaA).

An 8800 inductively coupled plasma triple quadrupole mass spectrometer (Agilent Technologies Inc., Santa Clara, CA, US) was used to quantify the trace elements: arsenic, barium, cadmium, cobalt, chromium, iron, manganese, lead, tin, strontium and vanadium. ICP-MS was equipped with a Micro-Mist glass concentric nebulizer, Peltier cooled double-pass Scott-type spray chamber, and Ni cones. The acquisition parameters were 1550 W RF power, 8.0 mm sampling depth, 15 L min^{-1} plasma gas, 1.03 L min^{-1} carrier gas, with the spray chamber temperature set at 2 °C; the isotopes measured were ^{75}As, ^{137}Ba, ^{111}Cd, ^{59}Co, ^{52}Cr, ^{56}Fe, ^{55}Mn, ^{208}Pb, ^{118}Sn, ^{88}Sr, and ^{51}V and the signals were collected using single-quad scan in the no gas mode, He mode and He–He mode with respectively 0, 4.5, and 10 mL min^{-1} flow in the collision cell. The integration time was 0.1 s for each mass value and data acquisition was established at 3 replicates and 100 sweeps for replicates. The samples were diluted at least at a 1 : 10 ratio with 1% HNO_3 and 0.5% HCl (37%, Superpure, Carlo Erba Reagents) in ultrapure water. Multielement standard solution for ICP (Merck) was used to prepare the calibration curves.

An Optima 3100 XL inductively coupled plasma-optical emission spectrometer (ICP-OES, PerkinElmer Inc., Shelton, CT, U.S.) was employed to quantify the following elements: Al (308.215 nm), Ca (315.887 nm), Mg (279.077 nm), P (214.914 nm), Se (196.026 nm), and Zn (213.857 nm), reported with analytical lines for quantitative determination. The ICP-OES was equipped with an axial torch, a segmented array charge-coupled device (SCD) detector and a Babington-type nebulizer with a cyclonic spray chamber for sample introduction; the work conditions of plasma were: an RF power of 1.40 kW, flow rates of 15 L min^{-1} and 0.5 L min^{-1} for the auxiliary gas; and a flow rate of 0.65 L min^{-1} for the nebulizer gas. Multielement and P standard solutions 1000 mg L^{-1} (Carlo Erba Reagents S.r.l) were used to obtain the calibration curves.[22]

Na and K were detected using an Analyst 800 atomic absorption spectrometer (AAS, PerkinElmer Inc., Shelton, CN, USA) in the emission mode at 766.5 nm and 589.0 nm, respectively. AAS working conditions were as follows: air flow at 17.0 L min^{-1}, acetylene flow at 2.0 mL min^{-1}, and integration time of 3 s for 3 replicates. Na and K standard solutions at 100 mg L^{-1} (Merck) were used to obtain the calibration curves. Minerals were expressed as mg kg^{-1} WM[23]

Amino acid profile. 0.2 g of freeze-dried oyster was weighed and mixed with 10 mL of HCl 6 M (37%, Superpure, Carlo Erba Reagents) into a tetrafluoro–methoxyl vessel and hydrolyzed by microwave digestion (Ethos Easy Advanced Microwave Digestion System equipped with an SK15 rotor). The hydrolyzed samples were then filtered (Whatman 589/2), dried under a nitrogen flow in a bath at 50 °C and finally resuspended in 0.1 M HCl (Merck). Amino acid detection and quantification were performed using a High Performance Liquid Chromatography (HPLC) system coupled with a fluorescence detector (Agilent Technologies 1260 Infinity). The chromatographic conditions used were in accordance with a method described by Agilent with some modifications.[24] The mobile phase A was 50 mM Na_2HPO_4 (Carlo Erba Reagents) in ultrapure water (MilliQ®, Merck KGaA), adjusted to pH 7.5; while mobile phase B was acetonitrile/methanol/ultrapure water, 45 : 45 : 10 vol% (VWR International Srl, Milan, Italy; Merck). 14 μL of hydrolyzed samples (diluted 1 : 20) or a standard amino acid mixture were added to 280 μL of 0.1 M borate buffer, pH 10.2 (Merck), 14 μL of internal standard, 140 μL of OPA (*o*-phthaldialdehyde) 1 mg mL^{-1} (P0532, Merck) as a derivatization agent and brought up to 1 mL with water. Tryptophan (T0254, Merck) was used as the internal standard, because during acid hydrolysis, tryptophan and cysteine were destroyed.[25,26] 20 μL of each sample was injected into a Pursuit XRs 5 C18 150 × 4.6 mm column at 20 °C, with detection at $\lambda_{excitement}$ = 230 nm and $\lambda_{emission}$ = 450 nm. The separation was performed at a flow rate of 0.7 mL min^{-1} employing a solvent gradient (vol%) as follows: 0 min 2% mobile phase B, 2.5 min 2% mobile phase B, 40 min 60% mobile phase B, 45 min 100% mobile phase B, and 50 min 100% mobile phase B, pre-equilibrated under initial conditions for 15 minutes. Appropriate amounts of standard amino acid solution 2.5 μmol mL^{-1} (AAS18, Merck) were used to obtain stock standard solutions from 25 to 700 pmol μL^{-1}, in triplicate. The calibration curves of each amino acid were obtained by plot-

ting the peak area against concentration, respectively (R^2 = 0.9935–0.9998). The amino acids analyzed were aspartic acid (15.56 min), glutamic acid (18.39 min), serine (24.84 min), histidine (25.19 min), arginine (26.88 min), glycine (28.23 min), threonine (28.47 min), alanine (31.42 min), tyrosine (32.07 min), valine + methionine (39.00 min), tryptophan (39.57 min), phenylalanine (41.15 min), isoleucine (42.66 min), leucine (43.48 min) and lysine (45.82 min). Amino acids were expressed as mg g^{-1} of WM.

Total polyphenol, carotenoid and flavonoid assays. The total polyphenol contents of oyster tissue were determined by using the Folin–Ciocalteau method.[27] The principle of the method is based on forming a blue-colored compound between phosphotungstic acid and polyphenols, in an alkaline medium. The concentration of polyphenols was calculated using the calibration curve, prepared under the same conditions as those of the sample, using the absorbance values at the maximum absorption, located at 750 nm. To obtain the calibration curve, a stock solution of gallic acid at a concentration of 100 mg L^{-1} was used. The concentration was reported as mg gallic acid equivalent (GAE)g_{LW} (LW: freeze-dried weight). Quantitative determination of carotenoids (β-carotene) was performed spectrophotometrically at 460 nm, based on the methodology proposed by Suhnel *et al.*[28] The concentration of carotenoids was expressed as β-carotene equivalent per g_{LW}. Quantification of flavonoids was performed using an aluminum chloride colorimetric assay at 420 nm.[29] The flavonoid concentration was estimated using the calibration curve of rutin and, finally, the content of flavonoids was expressed as mg rutin equivalent (RE) per g_{LW}.

Cell culture and chemicals

Human colorectal adenocarcinoma cells, Caco-2 (from the American Type Culture Collection, ATCC, Rockville, MD, USA), were cultured in Dulbecco's Modified Eagle's Medium (DMEM), high glucose with L-glutamine and sodium bicarbonate (Microtech, Pozzuoli, NA, Italy) supplemented with 10% fetal bovine serum (FBS, EuroClone, Milan, Italy), 1% penicillin/streptomycin (Lonza, Milan, Italy), HEPES (HIMEDIA, Einhausen, Germany), and 1% non-essential amino acids (ACL006, Microtech). Caco-2 cells were maintained at 37 °C in 5% CO_2 and 95% air until 70–80% confluence. For TNF-α (Bio-Techne SRL, Milano, Italy) treatments, a solution of 15 ng mL^{-1} in sterile PBS was used. For treatment with freeze-dried *C. gigas* samples, Caco-2 cells were pre-treated with different concentrations of freeze-dried extract dissolved in absolute EtOH, starting from a stock solution of 100 mg mL^{-1}.

MTT viability assay

Cell viability after pretreatment with freeze-dried oyster extract was determined through the MTT [3-(4,5-dimethylthiazol-2-yl)-2,5-diphenyltetrazolium bromide] assay as previously described.[30] Caco-2 cells were seeded in 96-well plates at a density of 2×10^4 cells per well in 200 μL of medium and exposed to various concentrations of lyophilized oyster extract (1, 2.5, 5, 10, 25, 50, 100, 250, 500 and 1000 μg mL^{-1}) for 24 hours. The day after, the medium containing the treatments was removed, and 50 μL of serum-free media and 50 μL of MTT solution (0.5 mg mL^{-1}) were added into each well and incubated for 3 hours. Then insoluble purple formazan crystals were dissolved by adding 100 μL of DMSO (37 °C for 15 minutes). The samples were shaken for 5 minutes (at room temperature (RT), in the dark) and the absorbance of the solution was measured with a spectrophotometer at 590 nm, using 670 nm as the reference wavelength as previously described.[31] Finally, the results were presented as a percentage of viability *vs.* control cells.

Cell viability of Caco-2 cells using the Trypan blue assay

Caco-2 cells were seeded in 6-well plates at a density of 2.5×10^5 cells per mL. When the right confluence was reached, they were pre-treated with different concentrations of the oyster lyophilized and dissolved in absolute EtOH: 5 μg mL^{-1}, 50 μg mL^{-1}, and 500 μg mL^{-1} for 24 h and the cell viability was measured using the Trypan blue exclusion assay. Briefly, the cells were harvested, 10 μL of cells and 10 μL of Trypan blue were mixed, and the number of cells was counted with a hemocytometer (Neubauer chamber, Sigma-Aldrich Chemie GmbH Taufkirchen, Germany). The number of live cells (unstained) and dead cells (stained blue) were counted, and the cell viability was expressed as a percentage of living cells with respect to the total number of cells:

$$\text{Viable cells}\,(\%) = (\text{total number of viable cells per mL} / \text{total number of cells per mL}) \times 100.$$

Immunocytochemistry

Caco-2 cells were grown on coverslips at a density of 0.5×10^5 cells per mL in 24-well plates and treated with TNF-α 15 ng mL^{-1} for 30 min, 1 h and 2 h. Then, the cells were washed twice with PBS 1×, fixed in 4% paraformaldehyde (PFA) in PBS for 10 min at RT and permeabilized with 0.2% Triton X-100 in PBS for 10 min at RT. After further washes with 1× PBS, 2% BSA was added for 1 hour to saturate the nonspecific sites. The coverslips were incubated with NF-κB primary antibody (D14E12, #8242, Cell Signaling Techology, Danvers, MA, USA) 1 : 500 in 0.25% BSA/PBS overnight at 4 °C. The next day, samples were incubated for 1 h with fluorochrome-conjugated anti-mouse secondary antibody (Green Mouse A11029 Alexa Fluor 488; Thermo Fisher Scientific, Waltham, MA, USA) in 0.25% BSA/PBS. Nuclei were stained with 1 μg mL^{-1} DAPI (Sigma-Aldrich) for 10 min. Coverslips were mounted on glass slides using PermaFluor™ Aqueous Mounting Medium (TA-06-FM Thermo Fisher Scientific) and examined with an Axio Imager A2 microscope equipped with a Leica DFC350 FX camera (Carl Zeiss s.p.a, Milan, Italy) at 40× magnification. All images were quantified using ImageJ software.

Nuclear-cytosolic protein extraction

Caco-2 cells were seeded in 100 mm Petri dishes (3×10^6 cells) and allowed to grow to confluence. After pre-treatment with lyophilized oyster extracts (5 μL, 50 μL and 500 μL) for 24 h

and treatment with TNF-α (15 ng mL^{-1}) for 2 h, the cells were detached and centrifuged for 5 min. Afterwards, the supernatant was discarded and the pellet was washed with 1 mL of 1× PBS, transferred to 1.5 mL Eppendorf and centrifuged for 5 minutes at 500*g*. The pellets were resuspended in cytosolic extraction buffer containing 10 mmol l^{-1} HEPES (pH 7.9), 10 mmol l^{-1} KCl, 1.5 mmol l^{-1} $MgCl_2$, 0.3% Nonidet P-40, 0.5 mmol l^{-1} ditreitiol, 0.5 mmol l^{-1} phenyl-methylsulfonylfluoride (PMSF), protease and phosphatase inhibitor cocktails. The lysates were incubated for 30 min on ice and subjected to intermittent mixing every 5 min. Then, the pellets were disrupted using G27 syringes and centrifuged at 14 000 rpm for 15 min. The supernatant containing cytosolic proteins was stored at −20 °C. Pellets containing the nuclei were washed twice with cytosolic extraction buffer, centrifuged for 5 min at 4 °C at 14 000 rpm, suspended in nuclear extraction buffer containing: 20 mmol l^{-1} HEPES (pH 7.9), 0.6 mol l^{-1} KCl, 1.5 mmol l^{-1} $MgCl_2$, 20% glycerol, 0.5 mmol l^{-1} phenylmethylsulfonyl fluoride and protease and phosphatase inhibitor cocktails and disrupted using a G27 syringe. Samples were incubated for 90 min in a Digital Tube Revolver (Thermo Scientific) at 4 °C. Finally, the samples were centrifuged at 16 000*g* for 5 min to obtain nuclear protein fractions and stored at −20 °C, as previously described.[32] The protein concentration was determined using the Bradford protein assay (Bio-Rad Protein Assay; Bio-Rad Laboratories, Inc., Milan, Italy). 30 μg of proteins were loaded onto 10% polyacrylamide SDS gels, electroblotted onto nitrocellulose membranes and separated by molecular size. Membranes were incubated overnight at 4 °C under gentle rocking with primary antibodies diluted in TBS-T 0.5% non-fat milk. Primary antibody used: NF-κB p65 (D14E12, Cell Signalling, cat. 8242, diluted 1 : 750 in TBS-T 0.5% non-fat milk), α-Tubulin (sc-23948, Santa Cruz Biotechnology, Inc., Dallas, TX, USA, diluted 1 : 1000 in TBS-T 0.5% non-fat milk) and Lamin A/C (sc-376248, Santa Cruz Biotechnology, Inc. diluted 1 : 1000 in TBS-T 0.5% non-fat milk) were used as loading controls. The membranes were then incubated with horseradish peroxidase-conjugated secondary antibody for 2 h (anti-mouse 1 : 5000; cat. BAF007, Biotechne, Minneapolis, USA). The bound antibodies were detected by chemiluminescence using ECL WESTAR ETAC UL-TRA 2.0 kit reagents (cat. XLS075.0100, CYANAGEN, Bologna, Italy) and an Bio-Rad ChemiDoc™ imaging system (Bio-Rad Laboratories). Images of the bands were digitized and densitometric analysis was performed using ImageJ software.

Protein extraction and western blot assay

Caco-2 cells were seeded in 60 mm Petri dishes (0.8×10^6 cells) and, after treatments, the cells were lysed with 20 μL of lysis buffer containing RIPA buffer 1× (50 mM Tris (pH 7.5), 150 mM NaCl, 10% glycerol, 1% Nonidet P-40, 1 mM EDTA, 0.1% SDS, 5 mM *N*-ethylmaleimide), protease inhibitor cocktail (100 μL for a total volume of 1 mL) (SIGMAFAST™ Protease Inhibitor Tablets, Merck), β-glycerol phosphate (10 μL for a total volume of 1 mL), and orthovanadate (5 μL for a total volume of 1 mL). The lysates were incubated for 30 min on ice and subjected to intermittent mixing every 5 min; then the samples were centrifuged (13 000 rpm, 15 min at 4 °C) and the supernatants were collected. The protein concentration was determined using the Bradford protein assay (Bio-Rad Protein Assay; Bio-Rad). Equivalent amounts of boiled proteins (30 μg) were loaded onto SDS polyacrylamide gels and separated by molecular size. Then, proteins separated from the gel were transferred to nitrocellulose membranes and blocked for 90 min in Tris-buffered saline, pH 7.5, containing 0.5% Tween 20 and 5% non-fat milk. The membranes were incubated overnight at 4 °C with the primary antibody diluted in TBS-T 0.5% non-fat milk: COX-2 1 : 500 (#12282S; Cell Signaling Technology). The membranes were then incubated for 2 h with horseradish peroxidase-conjugated secondary antibody (anti-mouse 1 : 5000; cat. BAF007, Biotechne). Finally, β-actin (cat. A3854, Merck) was used as a loading control. The bound antibodies were detected by chemiluminescence using ECL WESTAR ETAC ULTRA 2.0 kit reagents (cat. XLS075.0100, CYANAGEN) and the Bio-Rad ChemiDoc™ imaging system (Bio-Rad Laboratories). Images of the bands were digitized and densitometric analysis was performed using ImageJ software.

NF-κB DNA binding activity

The binding of specific DNA sequences, called kB sites, by NF-κB was evaluated using the "NF-κB (p65) transcription factor assay" (Cayman Chemical, Michigan, USA) as previously described.[33] The NF-κB protein present in the nuclear extract of different samples was incubated with oligonucleotides containing specific sequences, immobilized on a 96-well plate. A secondary antibody conjugated with a horseradish peroxidase provided a colorimetric result, which was detected spectrophotometrically at 450 nm.

Caco-2 differentiation and transepithelial resistance (TEER) measurements

The Caco-2 cell line differentiates into polar monolayers on a microporous membrane after 21 days of culture. To create the monolayer, Caco-2 cells were seeded in Transwell 6-well plates, on Millipore filters (pore size 0.4 μm, surface area 4.71 cm^2, and diameter 12 mm) at a density of 3×10^5 cells per cm^2 with 0.5 mL culture medium on the apical side and 1.5 mL culture medium on the basolateral side. The medium was replaced every 3 days for the first 14 days and then every day until day 21 to build a confluent monolayer. At day 21, the Caco-2 monolayer was pretreated for 24 h with the freeze-dried oyster and for another 24 h with 15 ng mL^{-1} TNF-α. Then transepithelial electrical resistance (TEER) of differentiated Caco-2 cells was assessed using a Millicell ERS-2 resistance system (Millipore).

The TEER value was calculated as $TEER = (R_m - R_{blank}) \times A$, where R_m is the transmembrane resistance; R_{blank} is the intrinsic resistance of the cell-free medium and A is the surface area of the membrane in cm^2.

Scanning electron microscopy (SEM) of differentiated Caco-2 cells

The sample morphology, size, and distribution were evaluated by observation under an electron microscope. To analyze the

external morphology, the cells were fixed in 2.5% glutaraldehyde in cacodylate buffer for 3 h at 4 °C. Then, the cells were post-fixed in 1% osmium tetroxide for 2 h at 4 °C and dried in a graded ethanol series; the samples were then metalized by gold coating (Edwards Sputter Coating S150; Edwards High Vacuum International, Wilmington, MA, USA) and analyzed at 15–20 kV using a scanning electron microscope (Zeiss EVO 40) with a LaB_6 source.

Statistical analysis

Statistical analysis was conducted using GraphPad Prism 6 software (GraphPad Software Inc., La Jolla, CA). All values are expressed as mean ± standard deviation or mean ± standard error of the mean (SEM) and differences were considered statistically significant at $p < 0.05$. Statistically significant differences between treated and untreated cells were evaluated by one-way analysis of variance (ANOVA) followed by the Bonferroni *post hoc* test.

Results and discussion

Proximate composition and potential bioactives

Proximate composition refers to the nutritional composition of a substance, such as protein, lipid, and moisture contents.[34] Oysters harvested in Goro have been demonstrated to possess a chemical composition that is notably rich in bioactive compounds, which may contribute to their anti-inflammatory properties. Specifically, they exhibit a high concentration of peptides, alongside a particularly advantageous omega-3 to omega-6 ratio, as well as significant polyphenol and carotenoid contents. *C. gigas*, along with other oyster species, is recognized for its substantial protein and lipid contents.[35] In this study, the protein and lipid contents were found to be 9.77 ± 0.95% WM and 2.05 ± 0.01% WM, respectively (Table 1).

The concentration of polyphenols was found to be 3.63 ± 0.37 mg g_{LW}^{-1} (Table 2), which is considered promising for the treatment and/or prevention of inflammation and related diseases.[36] Oysters contain such bioactive compounds, with 3,5-dihydroxy-4-methoxybenzyl alcohol (DHMBA) being the most notable. Notably, a role of DHMBA was recently suggested in the prevention of inflammation-related bone loss, by decreasing the level of NF-κB p65 in osteoblastic cells and its promoter activity, indicating its potential therapeutic efficacy under inflammatory conditions.[37]

Table 1 Proximate composition of the soft tissue of adult-sized *C. gigas* harvested in Goro (Italy)

	Concentration (%)
Moisture	74.77 ± 0.42
Total lipids	2.05 ± 0.01
Total crude proteins	9.77 ± 0.95
Ashes	1.78 ± 0.03
Carbohydrates[a]	11.65 ± 0.99

[a] Carbohydrate content has been determined by calculating the difference from other nutrients. Data are mean ± standard deviation ($n = 3$).

Table 2 Bioactive concentration in the soft tissue of adult-sized *C. gigas* harvested in Goro (Italy)

Nutrient	Concentration
Total polyphenols (mg GAE per g_{LW})	3.63 ± 0.37[a]
Total carotenoids (mg β-car per g_{LW})	10.51 ± 0.76[a]
Total flavonoids (mg RU per g_{LW})	1.26 ± 0.03[a]

[a] Data are mean ± standard deviation ($n = 3$).

The carotenoid content was found to be 10.51 ± 0.76 mg g_{LW}^{-1}. Oysters obtain carotenoids from their diet by filtering various algae from seawater. Fucoxanthin, diatoxanthin, diadinoxanthin, and alloxanthin have been isolated from *C. gigas* meat,[38] along with some minor carotenoids.[39] These compounds offer various health benefits due to their antioxidant and anti-inflammatory properties and serve as precursors to vitamin A, which is essential for immune function, eye health, and cell growth.[40] Apart from sodium, which is naturally derived from seawater, the mineral composition primarily includes calcium and magnesium, with lower amounts of zinc (Fig. 1A).

These minerals are recognized for their crucial roles in human health, including blood pressure regulation, clotting, nervous and muscle function, immune system function, carbohydrate and protein metabolism, among other processes, all involved either directly or indirectly in tissue inflammatory responses.[41]

High concentrations of amino acids have been identified, with tyrosine present at the highest concentration (Fig. 1B). Although tyrosine is not inherently anti-inflammatory, it contributes to the inflammatory process through the synthesis of certain enzymes, such as tyrosine hydroxylase (TH), which can influence inflammation.[42] Additionally, compounds derived from or containing tyrosine, like *N*-(*E*)-*p*-coumaroyl tyrosine, have shown anti-inflammatory properties.[43] *C. gigas* also exhibits a high content of glutamic acid, which is typically classified as an "immunonutrient" due to its significant anti-inflammatory activity.[44] Glutamic acid, as well as histidine and glycine, inhibit NF-κB activation, IκBα degradation, CD62E expression and IL-6 production in HCAECs, suggesting that they may exhibit anti-inflammatory effects during endothelial inflammation.[45] Moreover, a synergistic anti-inflammatory effect of phenolic acid-conjugated glutamine–histidine–glycine–valine peptides derived from oysters has been recently reported.[46] We observed an intriguing fatty acid profile (Fig. 1C), which is beneficial for health. Oysters contain approximately 52.65% saturated fatty acids (SFAs), 20.65% monounsaturated fatty acids (MUFAs), and 28.26% polyunsaturated fatty acids (PUFAs). Palmitic acid is the most abundant SFA, while oleic acid is the most abundant MUFA. Notably, the content of eicosapentaenoic acid (EPA) is almost double that reported for other oyster species.[47,48] An ω3/ω6 PUFA ratio of 7.5 has been calculated in our samples. PUFAs are generally considered to offer different beneficial health effects. However, ω3 and ω6 PUFAs exert opposing effects on

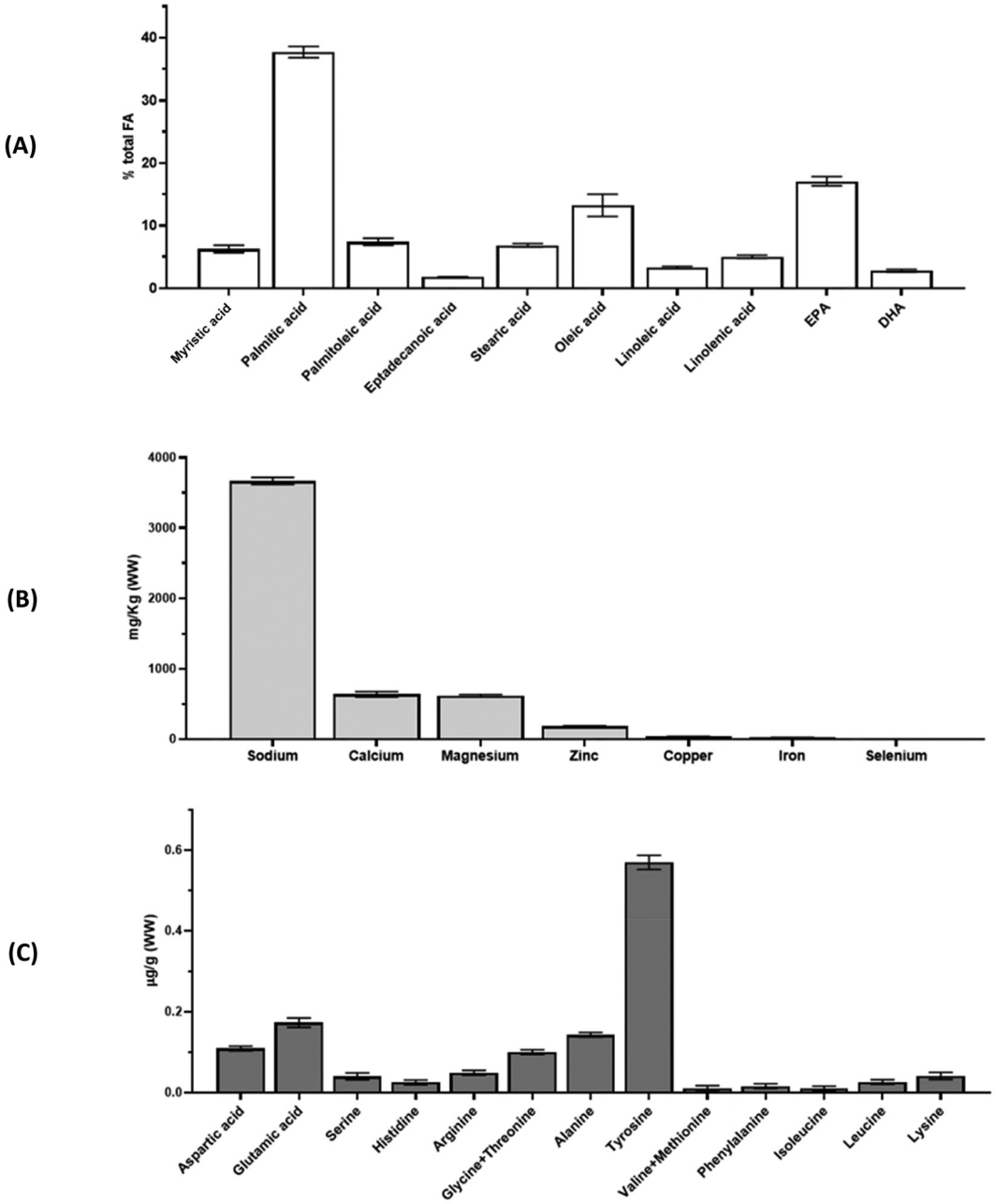

Fig. 1 Nutritional composition of commercial-sized *C. gigas* soft tissue: (A) fatty acid profile, (B) mineral composition and (C) amino acid content. Data are presented as mean ± standard deviation of three independent experiments. Quantification is shown in SI Tables (Tables S1–S3).

the body's metabolic functions, including inflammatory responses.[49] ω3 PUFAs aid in resolving inflammation and alter the function of vascular and carcinogenic biomarkers, playing a crucial role in the prevention and management of coronary disease, hypertension, and other inflammatory and autoimmune conditions.[50] They can form several potent anti-inflammatory lipid mediators (*e.g.*, resolvins and protectins) that collectively, directly or indirectly, suppress the activity of nuclear transcription factors, such as NF-κB, and reduce the production of pro-inflammatory enzymes and cytokines, including COX-2, (TNF)-α, and interleukin (IL)-1β.[51]

Effects of oyster extract treatments on Caco-2 cell viability

The possible anti-inflammatory properties of OE were tested in human intestinal epithelial cell line Caco-2, which is considered one of the main *in vitro* models used to study human intestinal barrier function.[52]

To choose the experimental doses of OE to be used in our study, we first analyzed their possible cytotoxic effects on Caco-2 cells by the MTT assay and Trypan blue exclusion assay. As shown in Fig. 2A and B, no cytotoxic effects were observed in Caco-2 cells treated for 24 h with OE at any of the tested

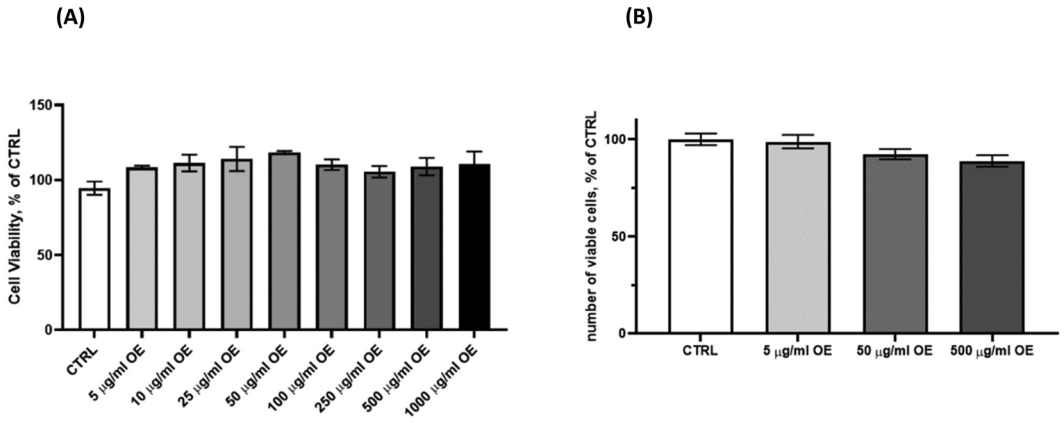

Fig. 2 Caco-2 cell viability after 24 hours of treatment with different doses of OE (from 5 μg ml^{-1} to 1000 μg ml^{-1}) evaluated by the MTT test (A) and the Trypan blue exclusion test (B). Data are presented as mean ± SEM of three independent experiments.

concentrations (from 5 to 1000 μg mL^{-1}). Therefore, we selected three different concentrations (5, 50, and 500 μg mL^{-1}) for the following experiments.

Time-dependent activation of NF-κB by TNF-α treatment in Caco-2 cells

To evaluate the anti-inflammatory effects of OE on Caco-2 cells, we focused on their role in preventing NF-κB activation in response to inflammatory stimuli. To induce NF-κB activation, and to simulate an inflammatory state in our *in vitro* model, Caco-2 cells were treated with two different stimuli: TNF-α and LPS from *Escherichia coli*. Caco-2 cells were poorly responsive to LPS stimulation (data not shown) due to the low expression of Toll-like receptor 4 (TLR-4); on the other hand, as depicted in Fig. 3A and B, the treatment of Caco-2 cells with TNF-α induced an increase in NF-κB nuclear translocation, especially after 2 h of exposure.

After TNF-α treatments, Caco-2 cells were stained for anti-NF-κB-FITC and DAPI for nuclear imaging (Fig. 3A), and intensity correlation between NF-κB and DAPI acquisitions was measured using Pearson's correlation coefficient (Fig. 3B). As depicted in Fig. 3B, we observed an increase in Pearson's correlation coefficient already at the earlier time point (30 min) reaching the statistical significance at 2 h after TNF-α treatment compared with untreated cells (CTRL). Therefore, based on this result, we decided to treat the Caco-2 cells with 15 ng mL^{-1} TNF-α for 2 h to induce an inflammatory response.

It is well accepted that a key event in the development and progression of various chronic inflammatory diseases of the human gastrointestinal tract is the activation of the nuclear factor kappa-light-chain-enhancer of activated B cells (NF-κB).[53] Nuclear factor (NF)-κB is a pleiotropic transcription factor that is normally sequestered in the cytoplasm in an inactive form by inhibitory proteins known as IκB.[54] Upon

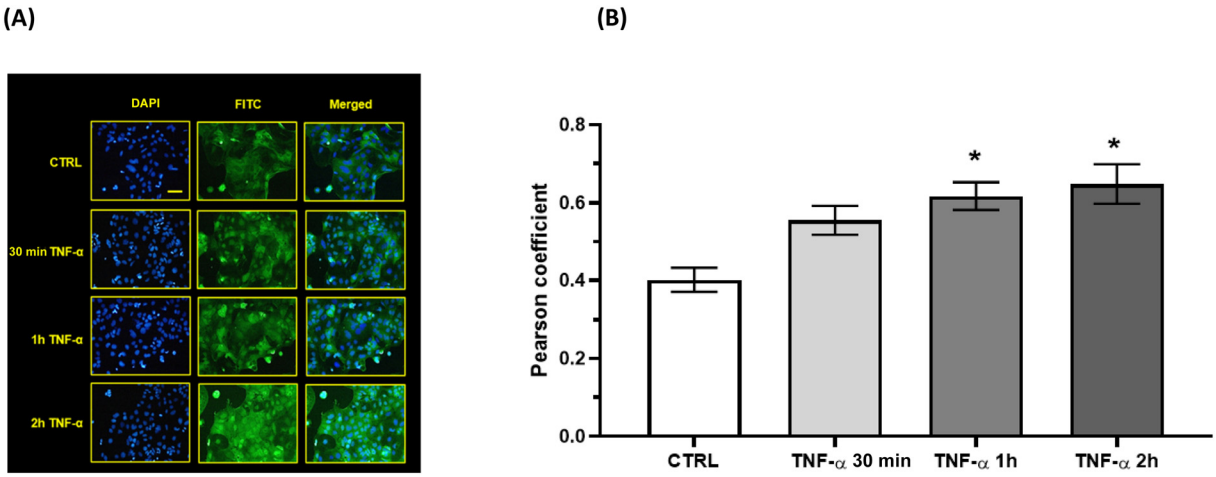

Fig. 3 (A) Representative images of NF-κB activation (green fluorescence in Caco-2 cells pre-treated for 30 min, 1 h and 2 h with 15 ng ml^{-1} TNF-α or untreated (CTRL)); nuclei are stained with DAPI (blue fluorescence). Magnification 40×. Scale bar = 20 μm. (B) Pearson correlation coefficient values for colocalization of NF-κB p65 and DAPI. Co-localization data are given as means ± SEM. ImageJ software was used for the analysis. Data are presented as mean ± SEM of three independent experiments. *$p < 0.05$ by one-way ANOVA; TNF-α treated cells *vs*. CTRL cells.

different stimuli, specific IκB kinase phosphorylate IκB promote their ubiquitination and degradation by the proteasome. Therefore, NF-κB can be activated, resulting in its rapid nuclear translocation, which leads to increased transcription of pro-inflammatory genes.[55] Therefore, establishing an inflammatory *in vitro* model based on NF-κB activation can help us to understand the possible anti-inflammatory properties of OE.

Oyster extract prevents TNF-α-induced NF-κB nuclear translocation in Caco-2 cells

The NF-κB family is composed of five members, NF-κB1 (or p50), NF-κB2 (or p52), RelA (or p65), RelB, and c-Rel. When activated, NF-κB migrates into the nucleus as dimers[56] and, in particular, the main NF-κB isoform induced by pro-inflammatory stimuli is the p50 : p65 dimer. Based on our previous results, we first treated Caco-2 cells for 24 hours with OE (5, 50, and 500 μg mL^{-1}), and then we exposed the cells to 15 ng mL^{-1} of TNF-α and finally, we evaluated NF-κB activation by western blot, *i.e.* the p65 expression level, in both cytoplasmic and nuclear cell compartments. No NF-κB nuclear translocation was observed in Caco-2 cells treated with OE (data not shown). As depicted in Fig. 4A, pretreatment with different concentrations of OE was able to prevent, in a dose-dependent fashion, the nuclear translocation of p65 after TNF-α stimulation. This effect reached statistical significance for OE higher doses (Fig. 4B). No statistically significant effect on p65 cytoplasmic levels was observed, suggesting that the effect is not at the transcriptional but rather at the post-translational level. This was confirmed in Fig. 4C, where the DNA-binding activity of p65 in Caco-2 challenged with TNF-α and pre-treated with OE is depicted. As clearly shown, while the OE alone did not significantly change the DNA-binding activity of NF-κB compared to the control condition, the pretreatment with OE

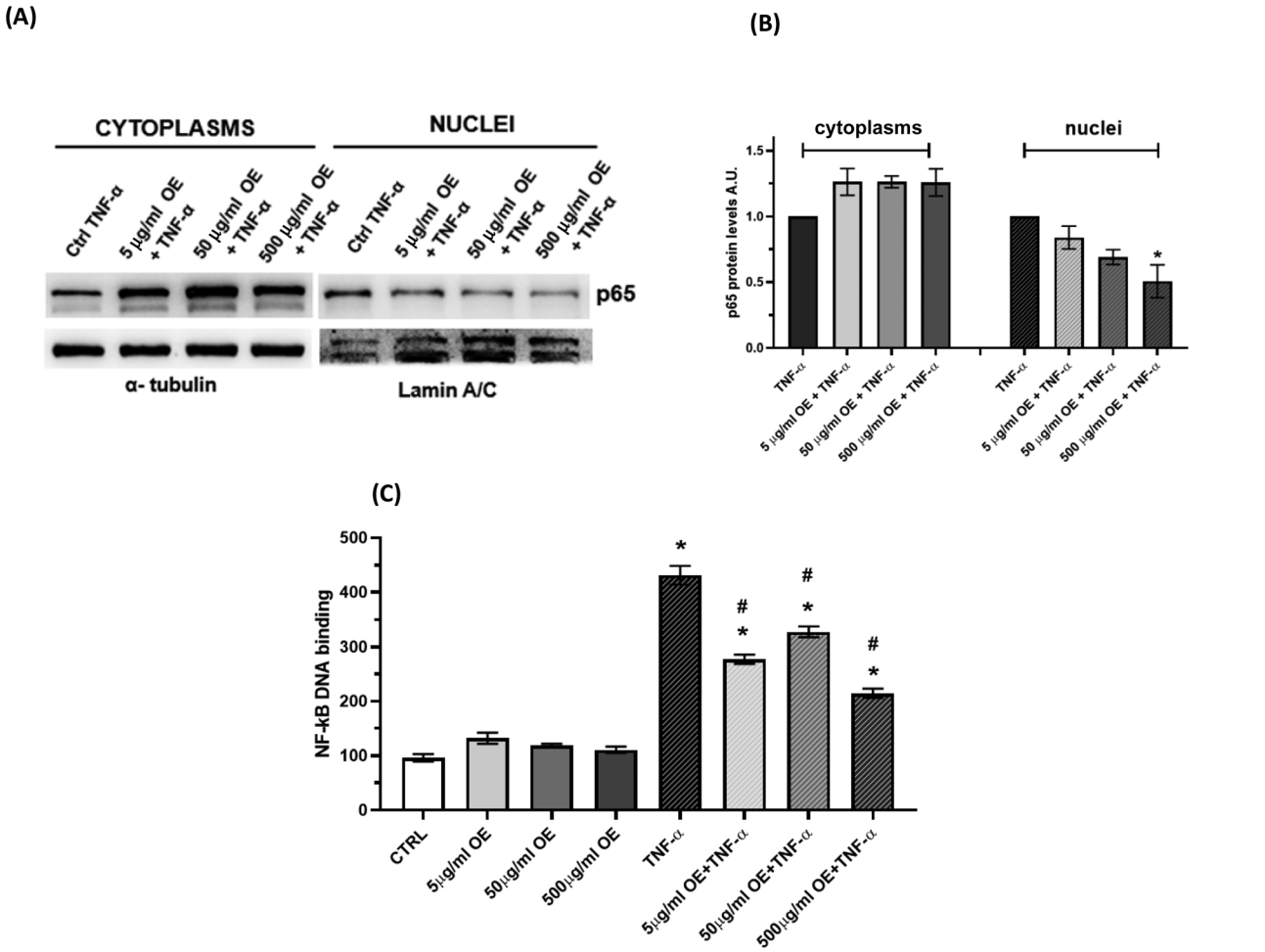

Fig. 4 Effect of oyster extract on NF-κB activation in Caco-2 cells. (A) Protein expression levels of the p65 subunit of NF-κB in the cytosol and nuclei of Caco-2 cells pre-treated for 24 hours with different concentrations of OE (5, 50 and 500 μg ml^{-1}) and then treated for 2 hours with 15 ng ml^{-1} TNF-α; (B) quantification of their expression levels. α-Tubulin and Lamin A/C were used as loading controls for cytoplasm and nuclei fractions, respectively. ImageJ software was used for the analysis. Data are presented as mean ± SEM of three independent experiments. *$p < 0.05$ by one-way ANOVA; OE treated cells *vs*. CTRL cells. (C) Effect of oyster extract on NF-κB DNA-binding in Caco-2 cells. The cells were treated for 24 hours with different doses of OE (5, 50 and 500 μg ml^{-1}) and then exposed for 2 hours to 15 ng ml^{-1} TNF-α. Data are presented as mean ± SEM of three independent experiments. */# $p < 0.05$ by one-way ANOVA; * treatment *vs*. CTRL; # TNF-α *vs*. OE + TNF-α.

strongly decreased (−35% 5 μg mL^{-1} OE *vs*. TNF-α; −26% 50 μg mL^{-1} OE *vs*. TNF-α; and −51% 500 μg mL^{-1} OE *vs*. TNF-α) the DNA-binding ability of activated NF-κB-p65, at all analyzed doses, especially at 500 μg mL^{-1} dose, in a statistically significant manner.

The potential of natural products derived from marine organisms to constrain NF-κB activation is exhaustively discussed and summarized by Folmer and colleagues.[57] In this paper, the authors describe the effects of natural marine products on molecular targets along the canonical NF-κB activation pathway; in particular, they argued that the natural marine compounds can act as NF-κB inhibitors with different mechanisms of action: targeting the enzymatic degradation of IκB, interfering with the activity of the 26S proteasome or inhibiting the DNA-binding of NF-κB. Moreover, in some cases, their mechanisms of action are still unknown to date. In this study, we were not able to fully elucidate the molecular mechanism responsible for NF-κB inhibition by OE treatment although it is possible that OE components can activate pathways that compete with NF-κB, such as the Nuclear factor erythroid 2-related factor 2 (NRF2) or Heme Oxygenase-1 (HO-1), and indirectly prevent its activation.[58]

The lack of a dose-dependent effect in the DNA binding results could be a consequence of missing some intermediate time points; nonetheless, the results can still clearly confirm OE's ability to prevent NF-κB activation.

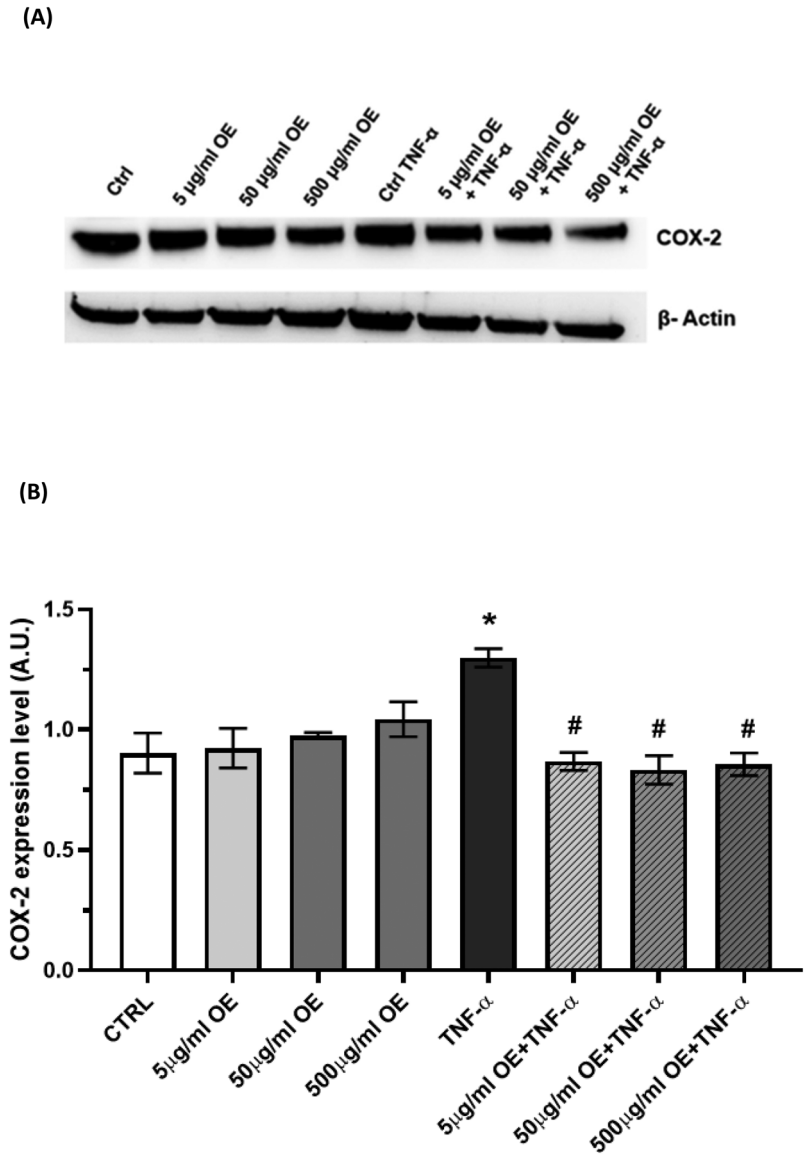

Fig. 5 Effect of oyster extract on the COX2 expression level in Caco-2 cells. (A) Protein expression levels of COX2 in Caco-2 cells treated for 24 hours with different doses of OE (5, 50 and 500 μg ml^{-1}) and then exposed for 2 hours to 15 ng ml^{-1} TNF-α; (B) quantification of the COX2 expression level. β-Actin was used as a loading control. ImageJ software was used for the analysis. Data are presented as mean ± SEM of three independent experiments. */# $p < 0.05$ by one-way ANOVA; * treatment *vs*. CTRL; # TNF-α *vs*. OE + TNF-α.

Oyster extract prevents COX-2 protein expression in Caco-2 cells

Activation of NF-κB is known to be involved in the regulation of the expression of numerous inflammatory genes, including those encoding TNF-α, IL-1β, IL-6, and cyclooxygenase-2 (COX-2), induced during the inflammatory process. Even though in this work we did not examine all the above-mentioned NF-κB-regulated genes, we observed a modulation of COX-2 protein expression levels upon OE pretreatment in TNF-α-inflamed Caco-2 cells. The COX-2 enzyme is induced by different inflammatory stimuli and converts arachidonic acid to prostaglandins, whose levels are normally elevated in inflamed tissues and are recognized to promote and propagate the inflammation response.[59] First, our results showed no effects on COX-2 protein level in Caco-2 cells stimulated with OE alone (Fig. 5A and B). Then, while TNF-α augmented the COX-2 expression level, the pretreatment with OE prevented this effect as established through statistical analysis of the protein quantification (Fig. 5B). This result agrees with previous studies demonstrating that different oyster-derived compounds exert modulatory effects on COX-2 level and/or activity.

In a recent work it has been demonstrated that β-thymosin, originated from the mantle of the Pacific oyster, *C. gigas* decreased the expression of COX-2 in LPS-induced RAW264.7 cells.[16] Siregar and colleagues demonstrated that the tyrosine-alanine (YA) peptide, the main component of *C. gigas* hydrolysate (OH), attenuates inflammatory signals in a mouse model of acute liver failure (ALF), by decreasing the enzymatic activity of COX-2.[17]

To the best of our knowledge, here we have shown for the first time that oyster tissue extracts exert an anti-inflammatory effect also on intestinal cells. Therefore, as well as being highly nutritious, they may also be considered nutritional supplements to alleviate intestinal inflammation associated with different chronic diseases.

Oyster extract prevents TNF-α-induced damage of intestinal epithelial barrier integrity

The intestinal barrier functionality is essential to maintain gut homeostasis and is tightly associated with intercellular structural integrity. The intestinal barrier is composed of a monolayer of epithelial cells connected by highly organized intercellular junctions: adherens junctions, desmosomes, tight junctions, and gap junctions. It has been proven that the impairment of intestinal barrier integrity results in spontaneous intestinal inflammation.[60,61] Then, to evaluate the protective effect of OE in maintaining gastrointestinal tract barrier integrity in our *in vitro* inflamed model, we measured the transepithelial electrical resistance (TEER) values, clear indicators of the cellular barrier status.

Specifically, to better analyze the protective effect of OE in the maintenance of this integrity, we used a differentiated Caco-2 monolayer that, due to its morphology and permeability characteristics, better mimics the human small intestine *in vitro* than undifferentiated Caco-2 cells.[62] As depicted in Fig. 6, we did not observe any differences in TEER values in differentiated Caco-2 cells pretreated for 24 h with OE compared to control cells.

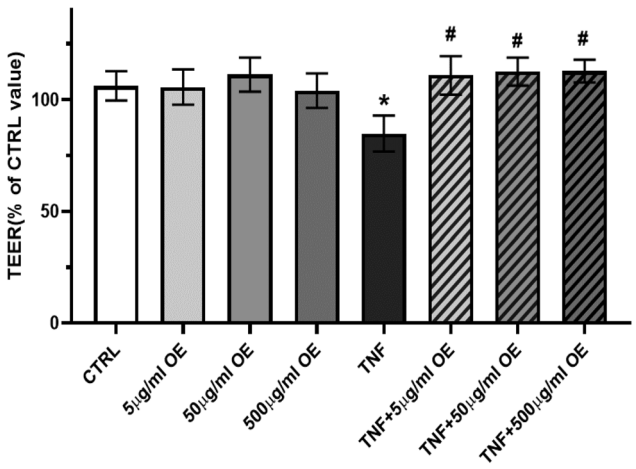

Fig. 6 Effects of TNF-α on the transepithelial electrical resistance (TEER) of 3D human intestinal tissues with or without OE pretreatment. Data are expressed as % *vs*. CTRL tissues (mean ± SEM of three experiments); * $p < 0.05$ by one-way ANOVA; * treatment *vs*. CTRL.

As expected, TNF-α caused a significant impairment in the permeability of the intestinal tissue by reducing TEER values, while the pretreatment with OE restored the TEER values to those of untreated samples. This result suggests that OE could contribute to preserving intestinal permeability under inflammatory conditions. Moreover, once again the TEER values measured highlight the protective role of OE in the gastrointestinal tract; several lines of evidence correlate the altered intestinal barrier function with different gastrointestinal pathologies, which require appropriate treatment, especially in prevention. Emerging evidence has demonstrated how marine-derived bioproducts may be excellent candidates and replacements for pharmacotherapy, due to their low toxicity and high content of bioactive peptides, polysaccharides, lipids, and more. In this scenario, *C. gigas* is an excellent source of proteins that can be hydrolyzed in different peptides characterized by high bioactivity. As far as we know, this is the first time that the beneficial effect of total oyster tissue extract has been observed in the maintenance of intestinal barrier integrity.

Oyster extract prevents intestinal epithelial morphological changes induced by TNF-α

Finally, the effects of OE on cell morphology were analyzed by scanning electron microscopy (SEM). CTRL cells and cells treated with 5, 50, or 500 μg mL^{-1} OE adhered tightly in a uniform layer, with no spaces between cellular edges; this result confirms that the general morphological characteristics of the monolayer and of the cell contact areas do not vary upon OE treatments compared to the control conditions (Fig. 7).

Conversely, the treatment of Caco-2 differentiated monolayer with TNF-α for 24 h induced structural alteration of the cell surface (Fig. 8A–C). After pretreatment with a low concentration of OE (5 μg mL^{-1}; Fig. 8D–F) the morphological aspect

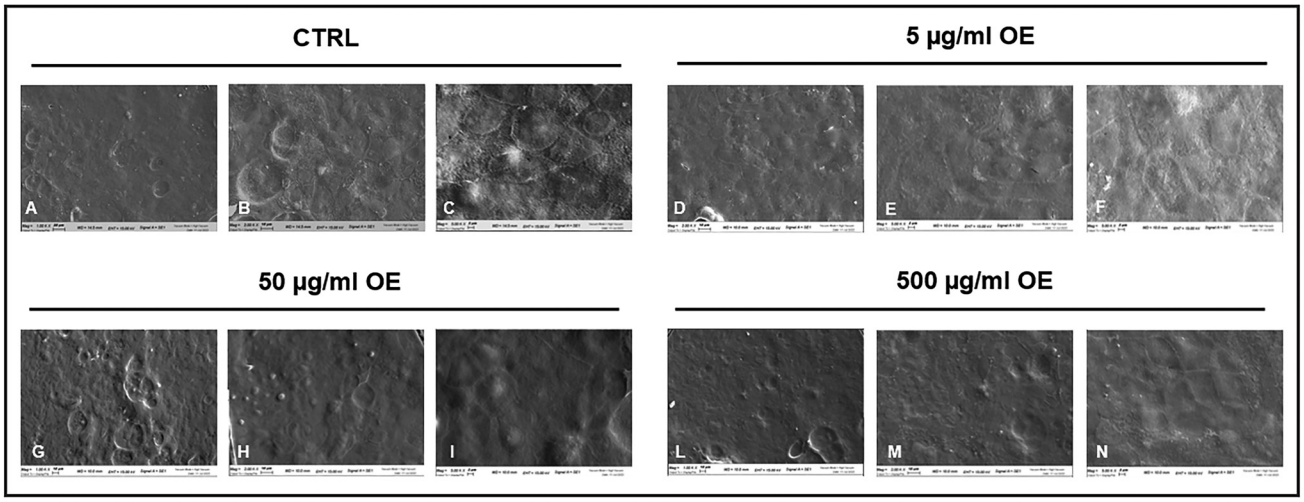

Fig. 7 Morphology of the Caco-2 monolayer exposed for 24 h to different doses of OE analyzed by SEM microscopy. The Caco-2 monolayer treated with different doses of OE (A, D, G, and L: 1k magnification; B, E, H, and M: 2k magnification; and C, F, I, and N: 5k magnification).

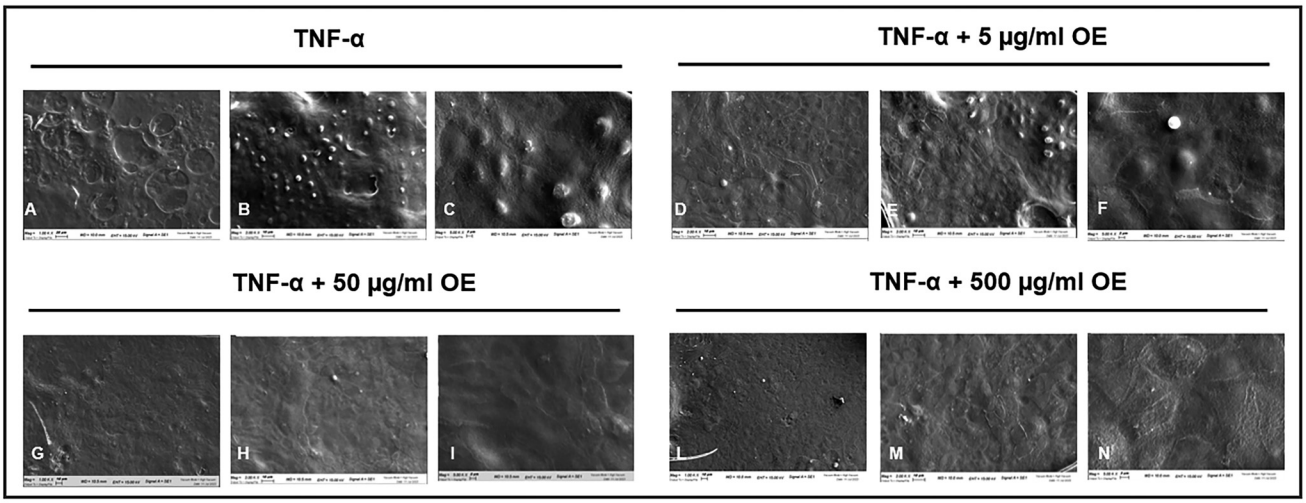

Fig. 8 Morphology of the Caco-2 monolayer exposed for 24 h to TNF-α with and without pre-treatment with different doses of OE analyzed by SEM microscopy. The Caco-2 monolayer treated with TNF-α for 24 hours, after pre-treatment with different doses of OE (A, D, G, L, 1k magnification; B, E, H, and M: 2k magnification; and C, F, I, and N: 5k magnification).

of the cells already appeared improved compared to those treated with TNF-α alone, even if some pyknotic–necrotic lesions were still present. Interestingly, upon pre-treatment of 24 hours with a high concentration of OE (50 μg mL^{-1} and 500 μg m^{-1}, Fig. 8G–N) the cell surface and cell-to-cell contacts are improved compared to TNF-α treated cells. Upon 500 μg mL^{-1} OE pretreatment the surface structural uniformity of the cell monolayer is almost restored despite the presence of an inflammatory agent. Consistent with the above-described changes in TEER values, this result again emphasizes how OE may prevent the intestinal barrier dysfunction.

Increasing evidence indicates that different bioactive food compounds may have anti-inflammatory effects in several tissues, including the intestinal mucosa. Recently, it has been suggested that marine organisms are an invaluable source of natural molecules and proposed as functional foods.[63] The recycling of oyster shells is nowadays considered a well-accepted sustainable solution. In contrast, the use of OE has received less significant interest although it is used as a dietary supplement since the 70's in the Far East for its beneficial properties.[64]

Conclusions

The final aim of this work was to pave the ground to produce oyster-based beneficial compounds with great potential for nutraceutical technology and/or possible applications in the food industry.

The Sacca di Goro is one of Italy's largest and most productive oyster farming areas. Despite the significant volume of shellfish produced, every year 30–40% of production has to be discarded as waste, due to small size, damaged shells, or deformities. Our work could potentially valorize these oysters for alternative nutraceutical applications, such as the production of nutritional supplements, and therefore reduce the amount of waste. We believe that promoting a more sustainable use of marine resources can provide additional economic opportunities for the local aquaculture industry.

Recent research has highlighted that the use of marine bioactives still faces several challenges; first, the challenges of the extraction process due to the complexity of the matrices due to different solubilities and stabilities of their compounds.[65,66] Additionally, regulatory constraints related to product approval and market authorization can be considered to guarantee the safety of the final marketed product. Besides these challenges, the unique bioactivities of marine-based products, especially antioxidant and anti-inflammatory properties, make them a promising resource for human health. These advantages highlight the importance of following this line of research and investing in innovative green technologies to foster the potential of marine-based compounds. In this scenario, our finding that oyster extract can reduce intestinal inflammation further supports the significance of marine bioactives as promising agents for human health. Therefore, overcoming the above-mentioned limitations in their use could support the discovery and realization of novel nutritional approaches.

We are aware that our study has been limited to *in vitro* cell experiments, which clearly need *in vivo* confirmation before extrapolating our results to real life, but we need to mention that using an *in vitro* model, although it does not fully recapitulate the complexity of living tissue, is a well-accepted approach for a first exploratory investigation aimed to understand the biological activities of these extracts.

Of course, the effective anti-inflammatory effects and safety of these compounds need to be confirmed through *in vivo* experiments and clinical trials before their possible nutraceutical use. Moreover, further studies are needed not only to specifically identify which ingredients of oyster tissue extract are more effective in inhibiting gut inflammation upon different external stimuli, but also to better evaluate the molecular mechanism by which OE modulates an inflammatory process.

Author contributions

Conceptualization and writing – original draft: MB and ET; data curation and methodology: MG, GT, DS, FCh, and FCe; supervision: LP and GC; and supervision and writing – review and editing: GV.

Conflicts of interest

There are no conflicts to declare.

Data availability

The data supporting this article are available upon request to the corresponding authors.

Supplementary information is available. See DOI: **https://doi.org/10.1039/d5fo02637g**.

References

1 L. Chen, H. Deng, H. Cui, J. Fang, Z. Zuo, J. Deng, Y. Li, X. Wang and L. Zhao, *Oncotarget*, 2017, **9**, 7204–7218.
2 Y. Y. Chow and K.-Y. Chin, *Mediators Inflammation*, 2020, **2020**, e8293921.
3 S.-F. Hendrayani, B. Al-Harbi, M. M. Al-Ansari, G. Silva and A. Aboussekhra, *Oncotarget*, 2016, **7**, 41974–41985.
4 X. Yu, A. M. Abd El-Aty, W. Su and M. Tan, *Food Saf. Health*, 2023, **1**, 22–40.
5 A. A. Manolis, T. A. Manolis, H. Melita and A. S. Manolis, *Curr. Med. Chem.*, 2022, **29**, 4050–4077.
6 Y. Mou, Y. Du, L. Zhou, J. Yue, X. Hu, Y. Liu, S. Chen, X. Lin, G. Zhang, H. Xiao and B. Dong, *Front. Immunol.*, 2022, **13**, 796288.
7 M. Chi, K. Ma, J. Wang, Z. Ding, Y. Li, S. Zhu, X. Liang, Q. Zhang, L. Song and C. Liu, *J. Immunol. Res.*, 2021, **2021**, e5516035.
8 S. Mondal, N. P. P. Soumya, S. Mini and S. K. Sivan, *Bioact. Compd Health Dis.*, 2021, **4**, 24.
9 F. Zhu, B. Du and B. Xu, *Crit. Rev. Food Sci. Nutr.*, 2018, **58**, 1260–1270.
10 R. Wall, R. P. Ross, G. F. Fitzgerald and C. Stanton, *Nutr. Rev.*, 2010, **68**, 280–289.
11 B. F. S. P. Negara, Md. Mohibbullah, J.-H. Sohn, J.-S. Kim and J.-S. Choi, *Int. J. Food Sci. Technol.*, 2022, **57**, 5732–5749.
12 E. Tamburini, E. A. Fano, G. Castaldelli and E. Turolla, *Resources*, 2019, **8**, 170.
13 H.-J. Lee, P. S. Saravana, Y.-N. Cho, M. Haq and B.-S. Chun, *J. Supercrit. Fluids*, 2018, **141**, 120–127.
14 S. Ulagesan, S. Krishnan, T.-J. Nam and Y.-H. Choi, *Front. Bioeng. Biotechnol.*, 2022, **10**, 913839.
15 M. Li, L. Qiu, L. Wang, W. Wang, L. Xin, Y. Li, Z. Liu and L. Song, *Fish Shellfish Immunol.*, 2016, **52**, 16–22.
16 D. Hwang, M. Kang, M. J. Jo, Y. B. Seo, N. G. Park and G.-D. Kim, *Mar. Drugs*, 2019, **17**, 129.
17 A. S. Siregar, M. M. Nyiramana, E.-J. Kim, S. B. Cho, M. S. Woo, D. K. Lee, S.-G. Hong, J. Han, S. S. Kang, D. R. Kim, Y. J. Choi and D. Kang, *Mar. Drugs*, 2021, **19**, 614.
18 Z.-J. Qian, W.-K. Jung, H.-G. Byun and S.-K. Kim, *Bioresour. Technol.*, 2008, **99**, 3365–3371.
19 J. M. Lynch and D. M. Barbano, *J. AOAC Int.*, 1999, **82**, 1389–1398.
20 N. Thiex, L. Novotny and A. Crawford, *J. AOAC Int.*, 2012, **95**, 1392–1397.

21 V. Brandolini, J. D. Coïsson, P. Tedeschi, D. Barile, E. Cereti, A. Maietti, G. Vecchiati, A. Martelli and M. Arlorio, *J. Agric. Food Chem.*, 2006, **54**, 9985–9991.
22 F. Chiefa, P. Tedeschi, M. Cescon, V. Costa, E. Sarti, M. Salgado-Ramos, N. Pallarés, N. D. Spadafora, L. Aguiari and L. Pasti, *Molecules*, 2024, **29**, 5546.
23 T. Chenet, G. Schwarz, C. Neff, B. Hattendorf, D. Günther, A. Martucci, M. Cescon, A. Baldi and L. Pasti, *Heliyon*, 2024, **10**, e29296.
24 P.-Y. Wang, F.-F. Shuang, J.-X. Yang, Y.-X. Jv, R.-Z. Hu, T. Chen, X.-H. Yao, W.-G. Zhao, L. Liu and D.-Y. Zhang, *Ind. Crops Prod.*, 2022, **186**, 115271.
25 P.-Y. Wang, F.-F. Shuang, J.-X. Yang, Y.-X. Jv, R.-Z. Hu, T. Chen, X.-H. Yao, W.-G. Zhao, L. Liu and D.-Y. Zhang, *Ind. Crops Prod.*, 2022, **186**, 115271.
26 M. Yang and S. A. Tomellini, *Anal. Chim. Acta*, 2000, **409**, 45–53.
27 H. S. Adegbusi, A. Ismail, N. Mohd Esa and Z. Azuan Mat Daud, Application of Folin-Ciocalteau colorimetric method in the determination of total tannin in maize and soybean food products. | EBSCOhost, **https://openurl.ebsco.com/contentitem/doi:10.47836%2Fifrj.29.5.13?sid=ebsco:plink:crawler&id=ebsco:doi:10.47836%2Fifrj.29.5.13**, (accessed April 23, 2025).
28 S. Suhnel, F. Lagreze, J. F. Ferreira, L. H. Campestrini and M. Maraschin, *Braz. J. Biol.*, 2009, **69**, 209–215.
29 A. M. Shraim, T. A. Ahmed, M. M. Rahman and Y. M. Hijji, *LWT–Food Sci. Technol.*, 2021, **150**, 111932.
30 L. Pozzetti, F. Ferrara, L. Marotta, S. Gemma, S. Butini, M. Benedusi, F. Fusi, A. Ahmed, S. Pomponi, S. Ferrari, M. Perini, A. Ramunno, G. Pepe, P. Campiglia, G. Valacchi, G. Carullo and G. Campiani, *Antioxidants*, 2022, **11**, 437.
31 M. Sguizzato, P. Mariani, F. Spinozzi, M. Benedusi, F. Cervellati, R. Cortesi, M. Drechsler, R. Prieux, G. Valacchi and E. Esposito, *Antioxidants*, 2020, **9**, 485.
32 R. Prieux, F. Ferrara, F. Cervellati, A. Guiotto, M. Benedusi and G. Valacchi, *In Vitro Cell. Dev. Biol.: Anim.*, 2022, **58**, 335–348.
33 M. Benedusi, E. Frigato, M. Beltramello, C. Bertolucci and G. Valacchi, *Mech. Ageing Dev.*, 2018, **172**, 13–20.
34 I. Ahmed, K. Jan, S. Fatma and M. A. O. Dawood, *J. Anim. Physiol. Anim. Nutr.*, 2022, **106**, 690–719.
35 B. F. S. P. Negara, M. Mohibbullah, J.-H. Sohn, J.-S. Kim and J.-S. Choi, *Int. J. Food Sci. Technol.*, 2022, **57**, 5732–5749.
36 A. Intharuksa, S. Kuljarusnont, Y. Sasaki and D. Tungmunnithum, *Molecules*, 2024, **29**, 5760.
37 S. Hobbs, M. Reynoso, A. V. Geddis, A. Y. Mitrophanov and R. W. Matheny, *Physiol. Rep.*, 2018, **6**, e13914.
38 S. Wan, Q. Li, H. Yu, S. Liu and L. Kong, *Gene*, 2022, **818**, 146226.
39 T. Maoka, K. Hashimoto, N. Akimoto and Y. Fujiwara, *J. Nat. Prod.*, 2001, **64**, 578–581.
40 P. Crupi, M. F. Faienza, M. Y. Naeem, F. Corbo, M. L. Clodoveo and M. Muraglia, *Antioxidants*, 2023, **12**, 1069.
41 I. Loaiza, C. Wong and V. Thiyagarajan, *J. Food Compos. Anal.*, 2023, **118**, 105159.
42 Z. Jenei-Lanzl, S. Capellino, F. Kees, M. Fleck, T. Lowin and R. H. Straub, *Ann. Rheum. Dis.*, 2015, **74**, 444–451.
43 Z. Jenei-Lanzl, S. Capellino, F. Kees, M. Fleck, T. Lowin and R. H. Straub, *Ann. Rheum. Dis.*, 2015, **74**, 444–451.
44 P. Jain and N. K. Khanna, *Agents Actions*, 1981, **11**, 243–249.
45 L. Zhong, L. Cao, R. Song, X.-F. Yang, J.-L. Li, H.-T. Yang, H.-X. Zhou and H.-T. Fan, *Sci. Rep.*, 2022, **12**, 11957.
46 S. Choi, S. Han, S. Lee, J. Kim, J. Kim and D.-K. Kang, *Antioxidants*, 2024, **13**, 447.
47 H. Saito, *Lipids*, 2004, **39**, 997–1005.
48 R. C. Martino and G. M. da Cruz, *Braz. Arch. Biol. Technol.*, 2004, **47**, 955–960.
49 R. K. Saini and Y.-S. Keum, *Life Sci.*, 2018, **203**, 255–267.
50 R. K. Saini and Y.-S. Keum, *Life Sci.*, 2018, **203**, 255–267.
51 J. X. Kang and K. H. Weylandt, in *Lipids in Health and Disease*, ed. P. J. Quinn and X. Wang, Springer Netherlands, Dordrecht, 2008, pp. 133–143.
52 M. D. C. Ponce de León-Rodríguez, J.-P. Guyot and C. Laurent-Babot, *Crit. Rev. Food Sci. Nutr.*, 2019, **59**, 3648–3666.
53 J. Van De Walle, A. Hendrickx, B. Romier, Y. Larondelle and Y.-J. Schneider, *Toxicol. in Vitro*, 2010, **24**, 1441–1449.
54 T. Matsusaka, K. Fujikawa, Y. Nishio, N. Mukaida, K. Matsushima, T. Kishimoto and S. Akira, *Proc. Natl. Acad. Sci. U. S. A.*, 1993, **90**, 10193–10197.
55 T. Liu, L. Zhang, D. Joo and S.-C. Sun, *Signal Transduction Targeted Ther.*, 2017, **2**, 1–9.
56 M. S. Hayden and S. Ghosh, *Genes Dev.*, 2012, **26**, 203–234.
57 F. Folmer, M. Jaspars, M. Dicato and M. Diederich, *Biochem. Pharmacol.*, 2008, **75**, 603–617.
58 V. Krajka-Kuźniak and W. Baer-Dubowska, *Int. J. Mol. Sci.*, 2021, **22**, 8223.
59 C. Yao and S. Narumiya, *Br. J. Pharmacol.*, 2019, **176**, 337–354.
60 C. Guo and J. Shen, *Clin. Rev. Allergy Immunol.*, 2021, **60**, 164–174.
61 M. V. Barone, R. Auricchio, M. Nanayakkara, L. Greco, R. Troncone and S. Auricchio, *Int. J. Mol. Sci.*, 2022, **23**, 7177.
62 X. Ding, X. Hu, Y. Chen, J. Xie, M. Ying, Y. Wang and Q. Yu, *Trends Food Sci. Technol.*, 2021, **107**, 455–465.
63 D. Lobine, K. R. R. Rengasamy and M. F. Mahomoodally, *Crit. Rev. Food Sci. Nutr.*, 2022, **62**, 5794–5823.
64 T. T. Nguyen, K. Heimann and W. Zhang, *Mar. Drugs*, 2020, **18**, 391.
65 A. Augusto, M. F. L. Lemos and S. F. J. Silva, *Appl. Sci.*, 2024, **14**, 8255.
66 I. Ahmed, M. Asgher, F. Sher, S. M. Hussain, N. Nazish, N. Joshi, A. Sharma, R. Parra-Saldívar, M. Bilal and H. M. N. Iqbal, *Mar. Drugs*, 2022, **20**, 208.